ASPECTS OF MACHINE INDUCED BACKGROUND IN THE LHC EXPERIMENTS

G.Corti and V.Talanov *, CERN, Geneva, Switzerland

Abstract

In our report we review different aspects of the LHC Machine Induced Background and their implication on the specific experiments. Based on different assumptions and estimates of the various parameters of the problem, we will present a few examples of the effect of this background on the experiments' detectors. Using the present understanding of the background sources and its formation in the machine structure, we provide indications on possible range of variation in the Machine Induced Background at various stages of LHC commissioning and operation.

INTRODUCTION

Products of the secondary cascades, initiated by proton losses upstream and downstream of the LHC interaction points (IP's), compose the *machine induced background* — the secondary radiation that reaches the zones of the experiments from the machine tunnel. The rate of this type of background is proportional to the machine beam current and depends on a given machine operating condition. Initial studies of the machine induced background at the LHC were presented in [1]. Since then significant progress was achieved in the understanding of this phenomenon.

SOURCES OF MACHINE INDUCED BACKGROUND

For a particular LHC interaction point, the total rate of the machine induced background depends on the contribution to the particle flux from secondary cascades, originating from sources that can be grouped as [2]:

- Inelastic and elastic interactions of the beam particles with the nuclei of the residual gas.
- Cleaning inefficiency which results in beam halo protons out-scattered and not absorbed in the collimation system but rather lost on the limiting apertures downstream of the cleaning insertions.
- Collisions in the interaction points, giving a fraction of the products that may reach the insertion region (IR) of the neighboring IP.

Secondary particles, produced in any of these sources, have different probability to reach a particular IP depending on where they originate with respect to the interaction point [3]. Inelastic and elastic scattering on the residual gas should be taken into account in the long straight section (LSS) of the given IP. From the general scheme of the

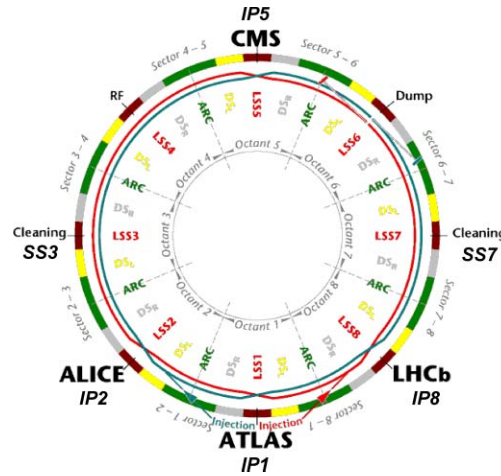

Figure 1: An overview of the LHC structure.

machine at Figure 1 one can conclude that elastic beam–gas scattering should be accounted for only on the length of the sectors between the given IP and the closest cleaning insertion. This cleaning insertion should absorb most of the upstream beam halo except for its part that will be lost at tertiary collimators in the experimental IR due to the cleaning inefficiency. The losses from one IP to another are relevant only for the case of influence of IP1 on the background in the IR2 and 8.

Numerical estimation of the machine induced background depends on the combination of the machine operation parameters, which in their turn may depend on each another [4]:

- Machine optics and apertures.
- Machine filling scheme.
- Residual gas density estimates.
- Cleaning inefficiency.

During the lifetime of the LHC, certain variations of these parameters are expected, some of them, like cleaning inefficiency, directly affecting the total background rates [5], some changing the background formation and dynamics [6]. To analyze the relative importance of these variations, different sources of the machine induced background should be evaluated separately with respect to each of the parameters.

In this report we present a set of snapshots of the machine induced background and its impact on the LHC experiments. The estimations in the experiments were done with the best available knowledge at the time of the studies, and they reflect the evolution of the understanding of

* On leave from IHEP, Protvino

background sources. Extrapolation and interpolation of the existing data can be based on the evaluation of expected variation of a given parameter of the calculations.

BACKGROUND IMPACT ON THE LHC EXPERIMENTS

With respect to the problem of the machine induced background we groups the LHC experiments in three categories: "general purpose" at high luminosity, dedicated physics experiments at lower luminosities and forward physics experiments at dedicated luminosities, running at specific machine conditions.

High Luminosity Experiments

High luminosity LHC experiments, ATLAS and CMS, will operate at the nominal luminosity of $L = 10^{34}$ cm^{-2}/s. The subdetectors of these experiments are well shielded down to a radius very close to the beam line from the secondary particle flux from the machine tunnel since there is a heavy shielding around TAS and Q1 at the LHC tunnel entrance to the experimental zones. As a result, the particle rates in the detectors from the machine induced background were estimated in the high luminosity experiments to give minor contributions to those due to the p–p collisions in nominal running conditions.

In ATLAS and CMS the impact of the machine induced background was estimated for different specific cases of the machine operation. In ATLAS, the hadron rates arriving from the machine tunnel are a factor ~ 25 lower than those predicted from the p–p collisions at the radius of EO Muon chamber [7]. In CMS Forward Muon system the rate of all particles but muons from the machine background was estimated to be 2–5 orders of magnitude lower than the background from the IP [8].

The inner or forward shielding of the high luminosity experiments is very effective in suppressing the hadron component of the background. However, a typical spectra of the machine induced background at the entrance to the experimental area [9] in Figure 2 shows a substantial number of muons with energy above a few GeV. This background component will not be fully attenuated by the shielding and may still affect the performance of the trigger in the experiments. Also a high energy hadron flux inside the unshielded beam aperture which will reach the region of the inner detectors of the experiments has to be evaluated accurately from realistic beam losses.

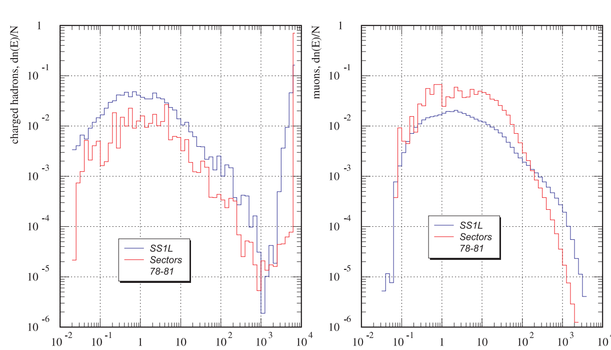

Figure 2: Spectra of charged hadrons (left) and muons (right), generated in the IR1 due to the proton losses along beam 1 in the SS1L (blue) and two upstream sectors of the LHC (red).

At the same time the use of the high energy muon component of the machine induced background is considered as one of the options for the commissioning of the experimental detectors. In ATLAS the study of muons from beam–gas interactions scaled to the case of machine operation with a beam current of 0.01 A gave the rate of 59 Hz in the MDT end-cap and 29 Hz in the MDT barrel [10], which was found significant and useful for the detector commissioning and alignment. Similar investigations are in progress in CMS [11].

Experiments at Lower Luminosities

Dedicated ion and B-physics experiments, ALICE and LHCb, will operate at the moderate luminosities of $L = 3\times10^{30}$ cm^{-2}/s and 2×10^{32} cm^{-2}/s. At the nominal LHC beam intensity the problem of the machine induced background can be considered more relevant for these experiments. Because of the low luminosity in the IP there is no TAS in front of the Q1 in the experimental zones of IP2 and 8 to provide shielding around the tunnel entrance that can absorb the machine induced background. Shielding in the low luminosity IR's will be installed inside the LHC tunnel [12].

	SPD1	SDD1	TPC
IP collisions	2000	190	2
Beam–gas around IP	250	12	0.05
Beam–gas in LSS	500	45	0.2
Total	2750	250	2.2

Table 1: Dose levels, [Gy] in the mid-rapidity region detectors of ALICE from the p–p and beam–gas sources of the background.

The effect of the machine induce background was analyzed in ALICE relative to the radiation levels from the p–p and Ar–Ar collisions [13]. An example of the obtained estimates for the dose levels in the mid-rapidity detectors are given in Table 1. These estimates were found to be a sizable contribution to the radiation levels in normal running conditions in several detectors. In LHCb the rates from the beam–gas induced background were investigated for different operation scenarios, with various beam current and residual gas pressures [14]. An overview of the estimated number of particles per bunch from the beam–gas background is given in Table 2. With the 31.5 MHz filled bunches the muon rate at the entrance of the LHCb cavern may vary from 34 MHz in the extreme conditions

<table>
<tr><th rowspan="4">Type of particle</th><th colspan="6">Particles per bunch</th></tr>
<tr><th colspan="3">(a) β^* = 1 m, I = 0.3 I_n</th><th colspan="3">(b) β^* = 10 m, I = I_n</th></tr>
<tr><th colspan="3">Ring 1
at -1 m from IP8</th><th colspan="3">Ring 2
at 19.9 m from IP8</th></tr>
<tr><th>Year 2
Beginning
(a)</th><th>Year 2
+10 days
(a)</th><th>Year 3
+90 days
(b)</th><th>Year 2
Beginning
(a)</th><th>Year 2
+10 days
(a)</th><th>Year 3
+90 days
(b)</th></tr>
<tr><td>muons</td><td>1.07</td><td>0.015</td><td>0.008</td><td>1.42</td><td>0.026</td><td>0.030</td></tr>
<tr><td>neutrons</td><td>3.43</td><td>0.065</td><td>0.059</td><td>5.09</td><td>0.185</td><td>0.423</td></tr>
<tr><td>p + π + K</td><td>7.68</td><td>0.133</td><td>0.104</td><td>8.54</td><td>0.194</td><td>0.304</td></tr>
<tr><td>Total</td><td>12.18</td><td>0.213</td><td>0.171</td><td>15.05</td><td>0.405</td><td>0.756</td></tr>
</table>

Table 2: Rates of the background components at the IP8, [particles/bunch] for the LHC Ring 1 and 2, two options of β^* in the IR8 and three cases of the residual gas pressure at different stages of the machine operation.

of the beginning of start-up up to 252 kHz after 10 days, for the losses upstream from the IP8 along the LHC Ring 1. The rates strongly depend on the machine running conditions. The estimated contribution of the machine induced background to the LHCb L_0 muon trigger bandwidth (fixed at 200 kHz) varies from $\sim 6\,\%$ to the whole output bandwidth in the extreme conditions of the first day. The loss in the trigger efficiency in the LHCb was estimated to be from few to several percents, when the machine background was combined with the background from the p–p interactions [15].

Estimates in both ALICE and LHCb were performed without shields in the tunnel around the experimental IP's and actually served as a proof for the need of the background shielding in the IR2 and 8. The estimates were performed with residual gas pressures where no NEG coating of the warm sections was assumed [16].

Beam–Gas in the Experimental Beam Pipes

A part of the machine related background which will be present in all the four LHC experiments mentioned above will come from the beam interactions with the residual gas nuclei inside the vacuum chamber directly within the experimental region. An example of the expected residual gas pressure profile in the experimental beam pipe is given in Figure 3, for the LHCb vacuum chamber in nominal machine operation. In the region of the LHCb VELO detector the average H_2 equivalent gas densities will be about $4{\times}10^{12}$, $2{\times}10^{12}$ and 10^{12} mol/m^3, for H_2, CO_2 and CO. Under these conditions, about 1 kHz of inelastic interactions is expected on the length of 120 cm of the VELO detector. Ongoing analysis of this background includes an investigation of its effect on the vertex trigger for the cases when these interactions, occurring together with the p–p collisions, could mimic secondary vertices and represent physics signatures [14].

Forward Physics Experiments

A set of Roman pot stations will be located for the purposes of forward physics measurements in the machine tunnel at both sides of the IR5 and are proposed for IR1. These detectors will operate at dedicated luminosities and during specific machine runs. They experience the machine background from the beam halo, beam–gas and beam–beam losses in the IP's. An example of the calculated background in the TOTEM station XRP3 at 220 m from the IP5 is given in Figure 4. The components of the background, induced by the beam–gas losses in the right part of IR5 on the outcoming beam 1 are shown in the scenario of machine oper-

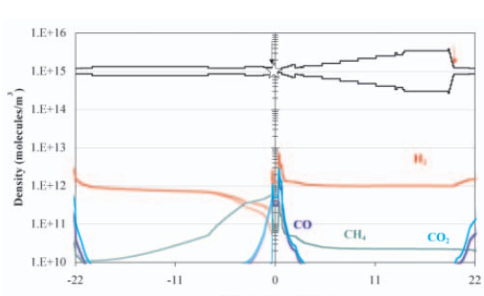

Figure 3: Pressure profiles, [mol/m^3] for different residual gas components in the LHCb experimental beam pipe (by A.Rossi, AT/VAC).

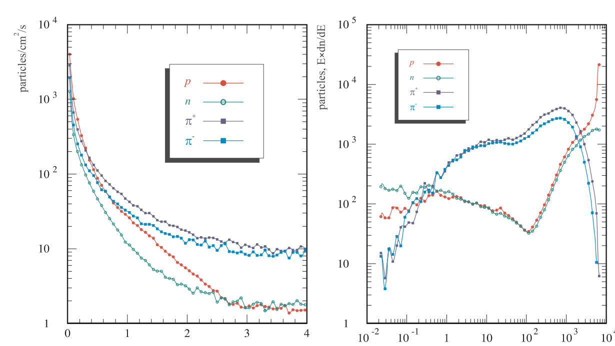

Figure 4: Particle flux density and particle spectra, calculated for the region of TOTEM station XRP3.

ation with 156 bunches and dedicated TOTEM optics [17].

The rates of the beam–gas background in the TOTEM stations were estimated to be of the same order of magnitude as those of the beam–beam, scaling particle fluxes in the detectors, calculated for the $L = 10^{33}$ cm^{-2}/s in IP5 [18], down to the 2×10^{29} cm^{-2}/s. Special techniques for the background analysis are being developed that already appeared effective in the rejection of the low energy and neutral components of the background [19].

EXPECTED VARIATION OF THE BACKGROUND

Estimations of the machine induced background in the experimental insertions depend on the machine operating conditions which define the relative contribution of different sources to the background. The rate of the background from the beam–gas losses depends directly on the residual gas pressure in the LHC sections, while the background from the particles out-scattered from the cleaning insertions is proportional to the cleaning inefficiency. Below we report the expected range of the variations for these quantities and evaluate the corresponding effect on the machine induced background rates.

Residual Gas Pressure in LSS's

Interactions of the beam with the residual gas nuclei from H_2, CO, CO_2 and CH_4 are the main source of beam losses in the LSS's. The resulting background depends on the absolute value of the density for a particular gas component and on the pressure profile in the structure of the straight section. An example of pressure profiles, calculated for the IR5 for two distinct cases of machine operation, are given in Figure 5. At machine start-up with the 0.2 A current and unconditioned surface of the vacuum chamber the maximal value for the H_2 equivalent gas density is expected to be at the level of 10^{14} mol/m^3 in the cold sections of the LSS. After a period of machine conditioning, in the nominal operation with the full current the maximal level of the gas pressure is expected to decrease to a few 10^{13} H_2 eq. mol/m^3. The level of the gas pressure in the warm sections of the LSS which have the NEG coating is predicted to be about two orders of magnitude lower respect to the cold sections in both cases.

n_b	43	156	2808
Start-up	1.8×10^{12}	5.7×10^{12}	4.3×10^{13}
Nominal	4.2×10^{11}	6.3×10^{11}	5.3×10^{12}

Table 3: Average H_2 equivalent residual gas density, [mol/m^3] in the IR1 & 5 at the machine start-up and at nominal operation after the machine conditioning with the beam of different intensity.

Average values for the residual gas density in the IR1 and 5, estimated for different scenarios of machine filling and operation [20] are given in Table 3. The average pressure at the machine start-up is expected to be ∼4–8 times higher then during machine operation with a conditioned vacuum chamber surface and maximal beam intensity. The comparison of the pressure profiles and gas density values available from the vacuum calculations shows that a variation of an order of magnitude may be expected in the level of the machine background induced by the beam–gas losses in the LSS's.

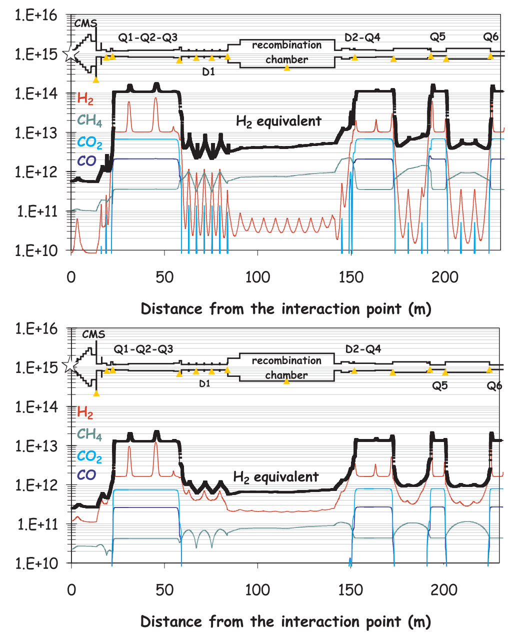

Figure 5: Pressure profiles, [mol/m^3] for different residual gas components in the CMS experimental insertion, for the machine start-up with the current of 0.2 A (top) and nominal operation with 0.56 A (bottom) (by A.Rossi, AT/VAC).

Gas Pressure in the Cold Sectors

The variation in the residual gas pressure in the cold sectors has a direct influence on the rate of the background at the entrance to the experimental areas. Figure 6 shows the rate of the particles, calculated as a function of the primary loss distance to the IP8, per unit of density of beam–gas interactions [2]. As can be seen from this Figure, the difference between the number of background particles, reaching the IP due to the beam–gas losses in the dispersion suppressor (DS) and the first arc cell (Arc), and those due to losses on the residual gas in the LSS itself is about 2–3 orders of magnitude. If the gas pressure in the cold DS and Arc will be more then 3 orders of magnitude higher then in the LSS, the beam–gas losses in these cold sectors will become the dominant source of the muon machine induced background.

The present estimate of the residual gas pressure in the cold sectors of the machine is the H_2 equivalent gas density of 10^{15} mol/m^3, which corresponds to the beam lifetime of 100 hours [21]. This number may be considered as

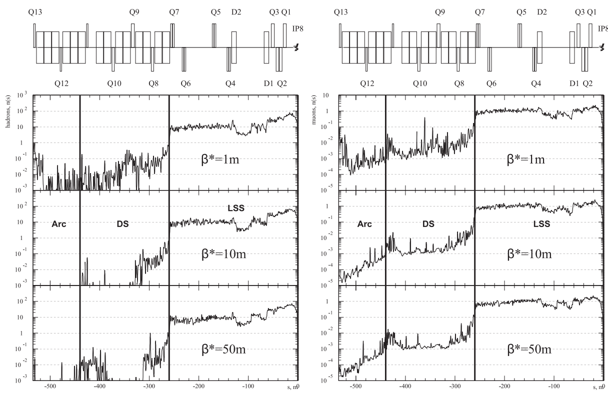

Figure 6: Number of hadrons (left) and muons (right), entering the UX85 cavern from the IP1 side, as a function of primary proton-nucleus interaction distance to the IP8, given per unit of linear density of beam-gas interactions, for three values of β^* in the IR8.

an upper limit for, obtained using a set of conservative assumptions on the beam screen pumping speed, photon critical energy and flux, and photon and photo-electron desorption. The resulting estimate is ∼20–30 times higher then the value for the residual gas density in the cold sections of the LSS's [22].

This assumption on the proportion between the gas density in the cold sections of LSS and arcs was used in the estimation of the machine induced background in the IR1 for the commissioning period with the tertiary collimators [9]. The calculated particle flux density at the entrance to the UX15 cavern is given in Figure 7, for the beam current of 0.01 A (43 bunches with 1.15×10^{11} protons/bunch) and a gas density in the 78 and 81 sectors a factor 30 higher than the corresponding value for Q6 in the LSS. It was found that under the given conditions the muon flux due to beam losses in the cold sectors becomes the dominant component, consisting of up to 80 % of the total muon flux from the machine background at the IP1.

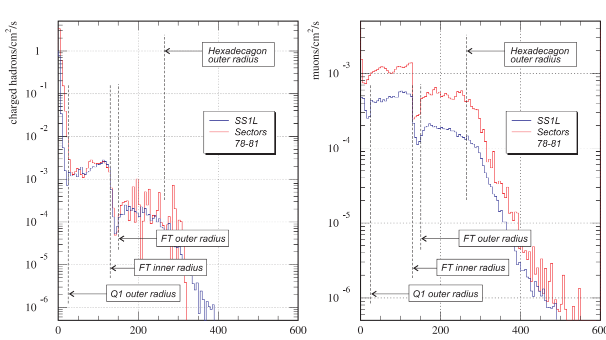

Figure 7: Density of the charged hadrons and muons flux [particles/cm^2/s] at the UX15 entrance due to the beam–gas losses in the SS1L (blue) and sectors 78–81 of the LHC.

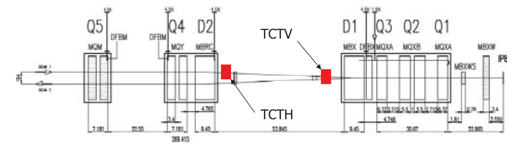

Figure 8: Layout of collimators on the IR7 side of IR8.

Collimation Inefficiency and Tertiary Halo

The design of the LHC collimation system has been changed recently with respect to what was used in the previous estimates of the machine induced background in the experimental insertions due to cleaning inefficiency [5]. The new collimation system includes two tertiary collimators at each side of the experimental insertions, a vertical one, TCTV, and a horizontal one, TCTH, to clean the tertiary halo in the IR's and provide additional protection to the superconducting magnets of the inner triplets [23].

An estimation of the tertiary background from the tertiary halo in the experimental insertion was made for the proposed configuration of the collimators in IR8, shown in Figure 8. The experimental insertion of IP8 is the closest IR downstream of beam 1 to IR7 and as such will experience the highest level of tertiary background. The simulations were based on the realistic maps of the losses on the TCT's, provided by the Collimation Project for the case of the tertiary halo originating from the collimators in IR7 and reaching IP8 in the direction of the LHC beam 1 [24].

	Charged hadrons	**Muons**
TCTV	5.9×10^6	1.8×10^6
TCTH	9.0×10^4	4.8×10^4
Total	6.0×10^6	1.9×10^6

Table 4: Background flux, [particles/s] for charged hadrons and muons, initiated by the vertical halo losses at the TCTV/H in the IR8.

Total values for the flux of charged hadrons and muons at the entrance to the experimental zone of IP8, initiated by these losses on tertiary collimators, as obtained in the cascade simulations, are given in Table 4. The results show that the losses in the vertical collimator TCTV are the major source of the tertiary background at IP8. Total flux values were compared with previous estimates for the beam–gas background [4] and were found to be of the same order of magnitude.

To evaluate the efficiency of shielding in IR8 with respect to this source of background, shielding walls in the tunnel were introduced in the calculations, according to the design given in Figure 9. The efficiency of the shielding is illustrated by the Table 5 which gives the total fluxes of the background components, initiated by the losses in TCT's but calculated with the shielding in the tunnel.

The presence of the shielding removes most of charged

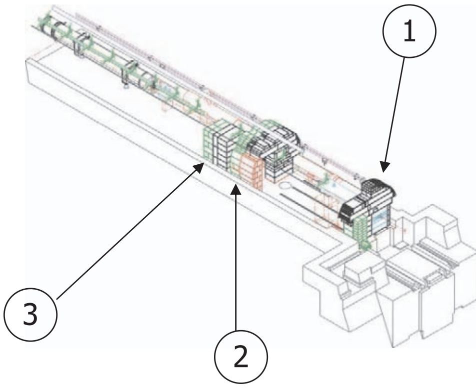

Figure 9: Layout of the shielding: 80 cm concrete wall (1), 80 cm iron plus 120 cm concrete wall (2) and chicane (3), in the tunnel upstream of IP8 in the direction of IR7.

hadron component of the background leaving only the particles inside the beam pipe aperture to reach the IP8 area. For the muons, a reduction factor of $\sim$ 2–3.5 was observed, depending on the position and type of collimator. Radial distributions of the particle flux density for the charged hadron and muon components of the background are given in Figure 10, for the cases with and without shielding. For comparison on the same Figure 10 are given the corresponding distributions of the beam–gas background components without shield, taken from [12]. For both charged hadrons and muons the radial distributions from these two background sources have significantly different shapes, with the beam–gas losses dominant at the low radii, around the beam line, while the tertiary background gives the main contribution at large distances from beam. For this reason the effect of shielding on the beam–gas rates is expected to be different.

	Charged hadrons	Muons
TCTV	6.2×10^4	5.1×10^5
TCTH	3.5×10^2	2.4×10^4
Total	6.2×10^4	5.3×10^5

Table 5: Tertiary background flux, [particles/s] for charged hadrons and muons, from the TCTV/H in the IR8, with the full shielding configuration.

The present calculations were done for the collimation beam lifetime of 30 h and under these conditions the level of the tertiary background was found comparable to the previously estimated beam–gas background levels. However, the flux of the tertiary background scales proportionally to the rate of the losses on the primary collimators, which increases with the decrease of the beam lifetime [25]. At beam lifetimes significantly lower than the assumed one, the tertiary background may become the main component of the machine induced background in the experimental insertions.

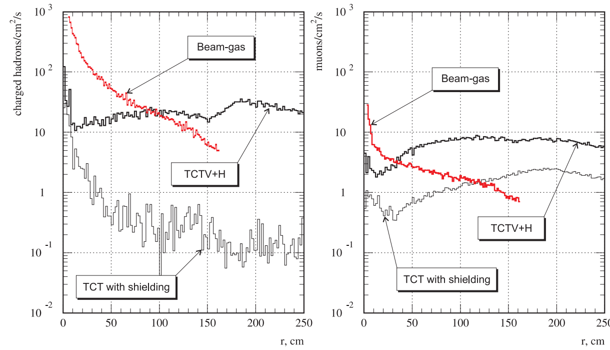

Figure 10: Particle flux density for charged hadrons and muons at the entrance to the UX85 cavern, for the background produced due to the losses in the TCTV and TCTH with and without shielding in the left part of the IR8, as compared to the previous beam–gas background estimates with no shielding plugs.

CONCLUSION

The impact of the machine induced background from the various sources of beam losses was evaluated in the LHC experiments for several different sets of the machine operation parameters. The impact of the background in the high luminosity experiments was found to be minor in the nominal conditions of operations. At the machine start-up period the background fluxes of this nature were found useful for the commissioning and alignment of the experimental detectors.

In the low luminosity experiments the presence of the machine induced background in the experimental regions may result in a contribution to the trigger bandwidth and in a loss of trigger efficiency. To suppress the background, shielding plugs will be installed in the machine tunnel around the low luminosity IP's. Special techniques for the background analysis and rejection are being developed in the forward physics experiments also.

Changes in the parameters of the machine operation may affect the total background levels and background formation. The changes in the residual gas pressure in the LSS's from the start-up during machine conditioning are expected to be of a factor $\sim$ 10. The estimates of the gas density for the cold parts are already conservative. Changes in both quantities will result in proportional changes of the total background fluxes in the IR's. Tertiary background due to the cleaning inefficiency was found to be of the same order of magnitude as the beam–gas background, for a collimation beam lifetime of 30 h. Lower beam lifetime will result in a significant increase of background, and in the case of a minimal beam lifetime the highest probable background levels will be observed.

ACKNOWLEDGMENTS

The authors are grateful to M. Deile, V. Hedberg, M. Huhtinen, A. Morsh and A. Rossi for their help in the

preparation of this talk.

REFERENCES

[1] K.M. Potter (editor). Proc. of the Workshop on LHC Backgrounds, CERN, Geneva, March 22, 1996.

[2] I. Azhgirey, I. Baishev, K.M. Potter *et al.*, “Methodical Study of the Machine Induced Background Formation in the IR8 of LHC”, LHC Project Note 258, CERN, Geneva, 2001.

[3] I. Azhgirey, I. Baishev, V. Talanov, “Machine Induced Background Sources Analysis for the IP1 Interaction Region of the LHC”, In: Proc. of RUPAC’2004, Dubna, 2004, p.511–513.

[4] I. Azhgirey, I. Baishev, K.M. Potter *et al.*, “Calculation of the Machine Induced Background Formation in IR2 of the LHC Using New Residual Gas Density Distributions”, LHC Project Note 273, CERN, Geneva, 2001.

[5] I. Baichev, J.B. Jeanneret, K.M. Potter, “Proton Losses Upstream of IP8 in LHC”, CERN LHC Project Report 500, Geneva, 2001.

[6] I. Azhgirey, I. Baishev, K.M. Potter *et al*. “Machine Induced Background in the Low Luminosity Insertions of the LHC”, CERN LHC Project Report 567, Geneva, 2002. Pres. at: 8th European Particle Accelerator Conference: a Europhysics Conference, La Vilette, Paris, France, 3–7 June 2002.

[7] V. Hedberg, “LHC Induced Background in ATLAS”, LHC Machine Induced Background Working Group meeting, CERN, Geneva, April 2005, `http://cern.ch/lhc-background.`

[8] A. Drozhdin, M. Huhtinen, N. Mokhov. NIM **A381** (1996) 531.

[9] V. Talanov, “Estimation of the Machine Induced Background for the Commissioning Period with Tertiary Collimators in the IR1 of the LHC”, CERN LHC Project Note 371, CERN, Geneva, 2005.

[10] M. Boonekamp, F. Gianotti, R.A. McPherson *et al.*, “Cosmic Ray, Beam–Halo and Beam–Gas Rate Studies for ATLAS Commissioning”, ATLAS Note GEN-001, CERN, Geneva, 2004.

[11] E. Barberis, P. Biallass, V. Drollinger *et al.*, “Trigger and Reconstruction Studies with Beam Halo and Cosmic Muons”, CMS Analysis Note 2005-046, CERN, Geneva, 2005.

[12] I. Azhgirey, I. Baishev, K.M. Potter *et al.*, “Evaluation of Some Options for Shielding from Machine Induced Background in the IR8”, LHC Project Note 307, CERN, Geneva, 2002.

[13] A. Morsh, “Machine Background in ALICE”, LHC Machine Induced Background Working Group meeting, CERN, Geneva, April 2005, `http://cern.ch/lhc-background.`

[14] G. Corti, “LHCb: Status of the Studies”, LHC Machine Induced Background Working Group meeting, CERN, Geneva, October 2005, `http://cern.ch/lhc-background.`

[15] E. Aslanides, F. Derue, R. le Gac *et al.*, “Performance of the Muon Trigger with a Realistic Simulation”, LHCb Note 2002-041, CERN, Geneva, 2002.

[16] I.R. Collins and O.B. Malyshev, “Dynamic Gas Density in the LHC Interaction Regions 1&5 and 2&8 for Optics Version 6.3”, CERN LHC Project Note 274, Geneva, 2001.

[17] V. Avati, M. Deile, D. Macina *et al.*, “First Results of the Machine Induced Background Estimation for the Forward Physics Detectors in the IR5 of the LHC”, CERN LHC Project Note 360, Geneva, 2004.

[18] A. Drozhdin, D. Macina, N. Mokhov *et al.*, “Accelerator Related Backgrounds in the LHC Forward Detectors”, In: Proc. of the PAC’2003, Portland, OR, May 12–16 2003, p.1742–1744.

[19] M. Deile, “Beam–Gas Background Studies for the TOTEM Roman Pots”, LHC Machine Induced Background Working Group meeting, CERN, Geneva, June 2005, `http://cern.ch/lhc-background.`

[20] A. Rossi, “Residual Gas Density Estimations in the LHC Insertion Regions IR1 and IR5 and the Experimental Regions of ATLAS and CMS for Different Beam Operations”, CERN LHC Project Report 783, Geneva, 2004.

[21] A. Rossi, “Expected Vacuum Performance in the Cold Arcs”, LHC Machine Induced Background Working Group meeting, CERN, Geneva, June 2005, `http://cern.ch/lhc-background.`

[22] A. Rossi, Private communication.

[23] R. Assmann, C. Fischer, D. Macina *et al.*, “Integration of Tertiary Collimators, Beam-Beam Rate Monitors and Space Reservation for a Calorimeter in the Experimental LSS’s,” LHC Project Document LHC-LJ-EC-0003, CERN, Geneva, 2004.

[24] R. Assmann, S. Redaelli, G. Rodert-Demolaize, “LHC Collimation System Studies Using SIXTRACK”, LHC Machine Induced Background Working Group meeting, CERN, Geneva, October 2005, `http://cern.ch/lhc-background.`

[25] R. Assmann, “Collimators and Cleaning: Could This Limit The LHC Performance ?” In: Proc. of the LHC Performance Workshop — Chamonix XII, 2003, p.163–170.